Computational Research Progress in Applied Science & Engineering

ISSN 2423-4591

CRPASE Vol. 04(04), 83-93, December 2018

Creep Analysis of the Autofrettage and Non- autofrettage Inconel 100 Super Alloy Thick-walled Spherical Pressure Vessel

Nabard Habibi*, Danial Wahdatpanah

Mechanical Engineering Department, Faculty of Engineering, University of Kurdistan

Keywords

Spherical vessel,
Creep,
Critical Pressure,
Autofrettage,
Stress-strain.

Abstract

As it is clear, one of the most challenging issues in the beams and spherical vessels are the creeps, which can have significant effects in temperature-dependent tests. This parameter is highly dependent on temperature and stress factors. It can be illustrated that we would use an analytical method and linearizing general creep equation namely Norton's law to extract relative constants (n, B) according to results and getting creep amount in a spherical pressure vessel in a non-autofrettage and then in an autofrettage mode by putting mentioned constants in non autofrettage and autofrettage stresses formula. It should be noted that the stress formulas in autofrettage mode are obtained by the linearization stress-strain curve in both elastic and plastic sections. The effects of autofrettage process in the entire spherical pressure vessel are observed at various pressures and temperatures, which can be seen in the following article. It can be concluded that applying the autofrettage process in the super-alloyed nickel thick-walled spherical vessel, reduces the creep amount by at least 10 times in the internal radius and 10000 times in the external radius of the vessel. By comparing creep values, we can observe that the autofrettage of spherical vessels is a very practical process in the prevention and immunization of thick-walled spherical vessels so that it can control or eliminate destructive actions such as creep.

Nomenclature

r: Radius of spherical vessel
r_i: Internal Radius of vessel
T_{r_i}: Internal radius temperature of vessel
E: Modulus of elasticity
E_{tu}: Tangent modulus (unloading state)
v: Poison's ratio
v^e: Equivalent poison's ratio
σ'_y: Unloading yield stress in compression
$\dot{\varepsilon}$: The secondary, steady-state or minimum creep rate
σ_e: The equivalent stress (the Von Mises stress)
Q_c: The creep initial activation energy
n: The constant value (dependent on the material properties)
$\dot{\varepsilon}_r$: Radial strain rate
ε_r^p: The plastic radial strain
ε_e^p: The plastic equivalent strain
$\sigma_{\theta_{aut}}$: The autofrettage circumferential stress
$\sigma_{\theta_{nor}}$: The non-autofrettage circumferential stress
σ_r^*: The ratio of radial stress in two states of the normal and autofrettage
σ_θ^*: The ratio of circumferential stress in two states of the normal and autofrettage
r_o: External radius of the vessel
r_c: Loading first yield radius of the vessel
T_{r_o}: External radius temperature of the vessel
E_t: Tangent modulus (loading state)
E_p: Plastic modulus
α: Coefficient of thermal expansion
σ_y: Loading yield stress in tension
$\dot{u}$: Derivation of displacement with respect to time
σ: The stress tolerated in the corresponding spherical vessel
A: A constant value proportional to the material property
T: The test temperature value in on ciliates
R: Ideal gas constant number of 8.314[27]
$\dot{\varepsilon}_e$: Equivalent strain rate
ε_θ^p: The plastic circumferential strain
$\sigma_{r_{aut}}$: The autofrettage radial stress
$\sigma_{r_{nor}}$: The non-autofrettage radial stress

* Corresponding Author:
E-mail address: n.habibi@uok.ac.ir – Tel, (+98) 8733660073 – Fax, (+98) 8733668513

Received: 13 August 2018; Accepted: 18 December 2018

1. Introduction

The spherical pressure vessels are one of the most important tools in engineering equipment, which have numerous applications. In the lifetime of spherical pressure vessels, there may be some flaws due to reasons such as corrosion, external object handling, fatigue loading, etc. Among these, the creep, or the strain rate, in the long run, can cause distortion, cracking or even failure. To solve this problem various solutions are presented. One way to reduce the creep is using the autofrettage process. The autofrettage process is achieved by thermal stresses. Autofrettage is known to induce residual stresses in the spherical vessels through exerting an initial pressure in a way that a part of the inner wall of the vessel enters into the plastic region. Through entering the vessels into the plastic area, the internal wall of vessel Getting into permanent deformation, after the autofrettage and unloading process, the plastic area does not tend to return to its original state, while the external part of the spherical vessels is in the elastic region, and pushes the inner area back to its original state. This causes tension in the spherical vessels. The created residual tension in the spherical vessels through autofrettage process is very important, which increases the pressure tolerate capacity of the spherical vessels and fatigue life, as well as the reduction of cracking and growth and decreases creep within it. Creep analysis in thick-walled spherical vessels is one of the most up-to-date and highly controversial issues in mechanic knowledge. In general, Inconel is a family of austenitic nickel-chromium-based super alloys. Inconel alloys are oxidation-corrosion-resistant materials well suited for service in extreme environments subjected to pressure and heat. When heated, Inconel forms a thick, stable, passivating oxide layer protecting the surface from further attack [1] .

Bhatnagar et al [2] calculated the creep stress and strain in the orthotropic thick-walled pressure vessels. Miller [3] offers a solution to stress and displacements in thick-walled spherical shells under radial and creep changes. Nayebi and Ali-abbadi [4] investigated the plastic cycle and creep behavior in thick-walled spherical vessels under pressure and temperature. Among these, the sphere, which has a thick-walled type and the nickel super alloy, is nickel called Inconel 100, and the thickness ratio to its radius is 0.375.

Through the results and data of the same kind in the creep experiments of the University of Swansea [5] on a beam, we can obtain some of the requirements for creep tests in spherical vessels. L. H. You and H. Ou [6] determine creep deformations and stresses in thick-walled spherical vessels with varying creep properties subjected to internal pressure. Parker[7] proposed an autofrettage process in open-end tubes.

Paolo Livieri and Paolo Lazzarin [8] provided a report of analysis of the appropriate analytical solutions for tension stresses in the autofrettage cylindrical vessels and the effect of residual stress in both the hardening and stress-strain curve forms. Thumse. Bergmann and Vormwald [9] did calculations of the residual stresses due to autofrettage process and the result of increasing the strength limit and they showed the large plastic penetration due to bending and the autofrettage process can reduce the stresses to a lesser extent than the yield stress in tension and pressure on both sides. In its method, Parker [10] provides an autofrettage model presented with regard to the strain relations and the Bauschinger effect based on stress-strain curve, tensile stress, material strain, and modified stress tolerance criterion. X. P Huang & W. C. Cui [11] showed an autofrettage model considering the material strain-hardening relationship and the Bauschinger effect, based on the actual tensile.

Parker and Huan [12] through numerical method solved the same problems for spherical vessels and steel thickener, creating an equivalent numerical solution for spherical vessels. In the elastic range, thermal stresses for spherical and cylindrical tanks are presented in [13-17]. In the other research [18], the behavior of spherical and cylindrical vessels under thermal and mechanical loads, a precise solution was used for the distribution of stress in thick-wall vessels. Through the fully elastic-plastic generator and stable conditions, temperature changes are obtained in a radial direction. Spherical vessels have been studied for different combinations of temperature, pressure and the ratio of the different radius in [19, 20]. The elastoplastic thermal stress is studied in spherical vessels under temperature variations around the wall thickness. Kargarnovin and co-workers [21] optimized the wall thickness in the thick-walled spherical vessels of the spherical shell through the concept of thermo-elastoplastic.

Davoudi Kashkoli and co-workers [22] assumed that the thermo-elastic creep response of the material is governed by Norton's law and material properties, except Poisson's ratio, are considered as a function of the radius of the spherical vessel, and an analytical solution is presented for calculation of stresses and displacements of axisymmetric FGM thick-walled spherical pressure vessels.

In the study of Gharechaei and loghman [23], time dependent stress and strain's redistribution of FGM spherical vessel and also homogeneous autofrettage spherical vessels has been investigated. This vessel is such considered that internal pressure in it is beyond the critical pressure and in result of internal pressure and temperature distribution some part of internal thickness of sphere will be plastically deformed. Thermo-elastic-plastic stresses are then developed in the vessel which is subject to change with time due to creep phenomenon. The loghman research [24] describes an analytical–numerical model developed for non-stationary electro-thermo-mechanical creep response of a smart sphere made of polyvinylidene fluoride (PVDF) using Burgers' creep model. The piezoelectric properties of the PVDF are used to control creep deformation of the sphere. Time-dependent stresses, displacements, electric potential and strains are calculated using Mendelson's method of successive approximation.

Time-dependent stress and deformation redistribution analysis of thick–walled spherical pressure vessels of FGM investigated [25]. Also, mechanical properties except poison ratio are considered to be the power function of the radial direction. In time dependent creep analysis, the total strain is a sum of mechanical, creep and temperature strains and these strains are functions of time and loading conditions. Liu and Shen [26] present analysis and experimental research on an autofrettaged pressure vessel with a cone and cylinder connection. Non-linear loading stresses and strains and the unloading resudial stresses and strains are considered. The residual stress and strain fields are obtained by the non-linear axisymmetric boundary element method (BEM).

In this research, an analytical analysis is performed, so at first, we consider a spherical vessel with arbitrary radius, and then the temperature-dependent parameters are obtained with linearizing the creeping equations (Norton), so that the general/total creep in the non-autofrettage mode in the cylinder spherical vessels is obtained. The creep problem can be proposed to provide an autofrettage mode. In order to obtain this result, we need to calculate the creep in the autofrettage mode in the spherical pressure vessel. This implies the elasticity modulus and the fact the shear modulus is stable Inconel alloys are oxidation-corrosion-resistant materials well suited for service in extreme environments subjected to pressure and heat. When heated, Inconel forms a thick, stable, passivating oxide layer protecting the surface from further attack [27-31]. In general, differences between this article and others are that we use rare superalloy that has never used in vessels and after that check the influences of autofrettage process on creep of the vessel and comparison amount of creep between normal and autofrettage mode.

2. Material Specification and Modeling

The material is considered a special nickel (super alloy) named Inconel 100, the composition percentage of the elements is as follows (Table 1).

Table 1. Inconel 100 Super Alloy Ingredients [32]

Cr	Co	Ti	Al	Mo	V	C	Zr	B	Ni
15	10	5.5	4.5	3	1	0.18	0.06	0.01	Bal.

Also, thick-walled pressure spherical vessel with inner and external radius 50 and 80 (*cm*) illustrated in Figure 1. Also, Inconel 100 Super alloy strain-stress curve is shown in Figure 2.

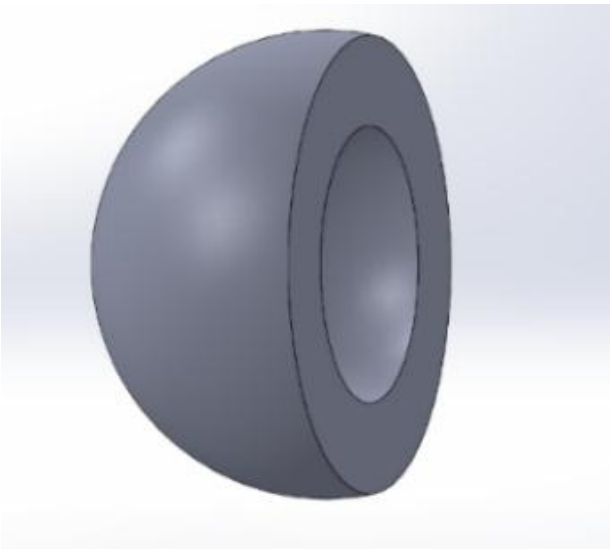

Figure 1. Thick-walled pressure spherical vessel with inner and external radii 50 and 80 (*cm*)

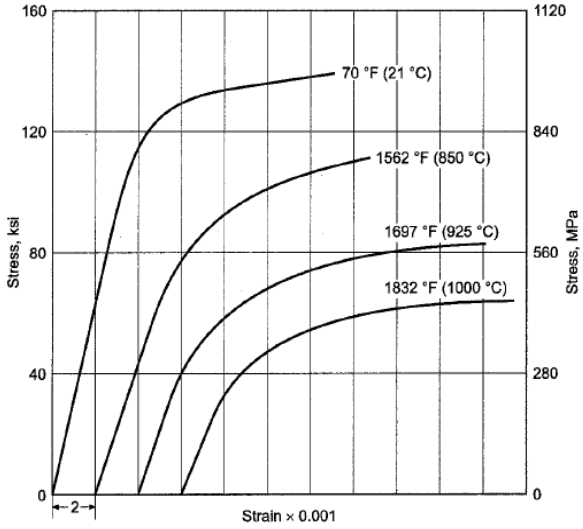

Figure 2. Inconel 100 Super alloy strain-stress curve [32]

3. Problem Solving

Norton equation is a basis for all the creep equations that gives us a non-linear relationship related to the temperature and stress in beams or vessels test. Norton's general equation can be seen in (1):

$$\dot{\varepsilon} = A\sigma^n \exp\left(-Q_c/RT\right) \quad (1)$$

where it can be seen, $\dot{\varepsilon}$ shows the secondary, steady-state or minimum creep rate, and σ is provided as the stress tolerated in the corresponding spherical vessels or beam. In addition, A is a constant value proportional to the material; Q_c is the creep initial activation energy, *T* is the test temperature value in on ciliates, *n* is the constant value, which is dependent on the properties of the material and R is ideal gas constant number of 8.314 [33], which is the molecular movement value at the desired temperature on Celsius. To simplify the equation, it is assumed that:

$$B = A \exp\left(-Q_c/RT\right) \quad (2)$$

So, the Norton creeping equation is simplified as following:

$$\dot{\varepsilon} = \mathrm{B}(r)\sigma^{n(r)} \quad (3)$$

Due to the internal pressure, the creep variations in the spherical thick-wall pressurized vessels in the steady state are symmetric. The geometric relationship between radial and circumferential strain rates with radial displacement rate is expressed as the Eq. (4-1). Also, it is shown in the following the relationship between the radial and circumferential strain rates with stresses for an isotropic unstable material (Eq. (4-2)).

$$\dot{\varepsilon}_r = \frac{d\dot{u}}{dr} = \frac{\dot{\varepsilon}_e}{\sigma_e}\left[\sigma_r - 0.5\left(\sigma_\theta + \sigma_\varphi\right)\right] \quad (4\text{-}1)$$

$$\dot{\varepsilon}_\theta = \frac{d\dot{u}}{dr} = \frac{\dot{\varepsilon}_e}{\sigma_e}\left[\sigma_\theta - 0.5\left(\sigma_r + \sigma_\varphi\right)\right] \quad (4\text{-}2)$$

where, $\dot{\varepsilon}_e$ is the secondary, steady-state or minimum creep rate in Table 2, σ_e, equivalent stress and σ_r ، σ_θ ، σ_φ are radial, longitudinal and transverse stresses, respectively. Due to symmetric of the sphere, circumferential stress replaced by transverse and longitudinal stresses, therefore, using Eqs. (4) and $\sigma_\theta = \sigma_\varphi$, result as following:

Table 2. Data obtained in different temperatures and tensions [5].

Stress (MPa) $\boldsymbol{\sigma_e}$	Temp (° C)	Minimum creep rate $\dot{\boldsymbol{\varepsilon}}_{\boldsymbol{e}}$ (10^{-9} s^{-1})	Rapture time (10^3s)	Rupture Strain (*10^{-1})
350	**800**	1.19	9671.9	0.2640
375		2.25	5444.9	0.2481
400		2.79	4374.0	0.2286
425		5.80	4301.7	0.5050
450		6.59	2391.8	0.2024
300	**850**	**5.37**	**3012.1**	0.5056
325		7.78	2343.1	0.3611
350		20.6	1029.9	0.4612
375		30.2	855.16	0.4076
400		53.2	313.83	0.2123
400		19.7	967.62	0.3671
200	**900**	**2.40**	**4986.4**	0.3748
225		6.15	2084.0	0.5551
250		16.6	1142.7	0.5714
250		15.5	1125.4	0.6047
275		9.85	1464.2	0.4035
300		49.6	466.36	0.4673
325		84.1	305.91	0.5099
350		377	76.75	0.3720
400		1150	27.692	0.3909
150	**950**	**4.23**	**2008.4**	0.4515
200		38.6	463.96	0.7029
250		298	95.547	0.8009
300		839	30.427	0.4010
200		120	219.06	0.7029

The variation of UTS value versus temperature is shown in Table 3. Also, Mean Coefficient of Inconel 100 at different temperatures illustrated in Table 4.

Table 3. The variation of UTS value versus temperature [5]

Temperature (°C)	800	850	900	950
UTS (MPa)	1000	887	773	660

Table 4. Mean Coefficient of Inconel 100 at different temperatures [32]

Temp °C	Temp °F	Mean Coefficient per °C (*10^{-4})
70-200	21.11- 93.33	0.1296
70-400	21.11-204.44	0.1296
70-600	21.11-315.55	0.1314
70-800	21.11-426.66	0.1350
70-1000	21.11-537.77	0.1386
70-1200	21.11-648.88	0.1440
70-1400	21.11-760	0.1496
70-1600	21.11-871.11	0.1584
70-1800	21.11-982.22	0.1674
70-2000	21.11-1093.33	0.1800

Specifications of Inconel 100 are considered acording to Table 5.

Table 5. Specification of Inconel 100 [32]

Temp °C	°F	Yield Strength of 0.2% (MPa)	Tensile Strength (MPa)	Elo %	Reduction of Area
70	21.11	848.05	1013.52	9.0	11.0
1000	537.77	882.52	1089.37	9.0	11.0
1200	648.88	889.42	1110.05	6.0	7.0
1350	732.22	875.63	1096.26	6.5	7.2
1500	815.55	813.58	992.84	6.0	7.2
1700	926.66	503.31	737.73	6.0	7.2
1900	1037.78	282.68	441.26	6.0	8.0

$$\dot{\varepsilon}_r = \frac{\dot{\varepsilon}_e}{\sigma_e}(\sigma_r - \sigma_\theta) \tag{5-1}$$

$$\dot{\varepsilon}_\theta = \frac{\dot{\varepsilon}_e}{2\sigma_e}(\sigma_\theta - \sigma_r) \tag{5-2}$$

So it can be concluded:

$$\dot{\varepsilon}_r = -2\dot{\varepsilon}_\theta \quad \Rightarrow \quad \dot{\varepsilon}_r + \dot{\varepsilon}_\theta + \sigma_\varphi = \dot{\varepsilon}_r + 2\dot{\varepsilon}_\theta = 0 \tag{6}$$

The equivalent stresses for spherical thick-walled spherical vessels are as Eq. (7)

$$\sigma_e = \frac{1}{\sqrt{2}}\sqrt{(\sigma_\theta - \sigma_r)^2 - \left(\sigma_\theta - \sigma_\varphi\right)^2 - (\sigma_\varphi - \sigma_r)^2} = \sigma_\theta - \sigma_r \tag{7}$$

The equivalent creep rate can be obtained from the equivalence crustal deformation, that is,

$$\sigma_e\dot{\varepsilon}_e = \sigma_\theta\dot{\varepsilon}_\theta + \sigma_\varphi\dot{\varepsilon}_\varphi + \sigma_r\dot{\varepsilon}_r \tag{8}$$

Now, using the results of H. You and H. Ou, [6], we can find out that by putting B, *n*, as a variable value, no change in the whole Norton equation will occur and the values for the solution in a given answer are changed relative to each other. Finally, from their findings, it can be said that *n* and B are given numerically independent of the spherical vessels radius. Therefore, we have:

$$\dot{\varepsilon}_e = B\sigma_e^n \tag{9}$$

According to the test data from the University of Swansea, which is listed in Table 2, from 800 ° C to 950 ° C, the necessary specifications to obtain the *n* and B constants are minimum creep rate $\dot{\varepsilon}_e$ and equivalent stress σ_e. Now we have to linearize Norton's mathematical model so that we can be able to obtain the constant values of *n* and B for the test temperatures (800, 850, 900, 950 Celsius).

The first step of linearization is getting log from Eq. (9). So, we can fit the values of stress and creep at any temperature, then a graph is depicted in terms of log-stress (MPa) versus log-strain rate (s^{-1}), a linear is obtained as $y = mx + c$. The second step is to fit the opposite values instead of the constants *B* and *n* into $m = n$ and $c = \log B$. The linearity gradient line of the Norton equation in the spherical pressure vessel at 800-950 °C illustrated in Figures 3-6.

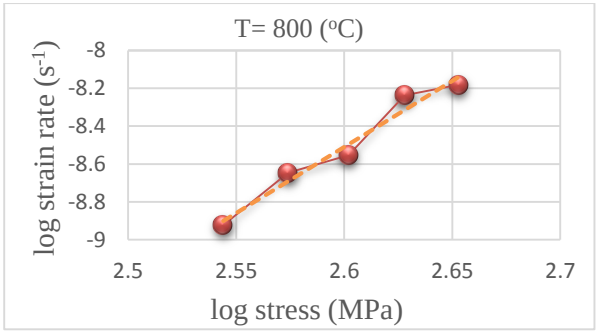

Figure 3. The linearity gradient line of the Norton equation in the spherical pressure vessel at 800 °C

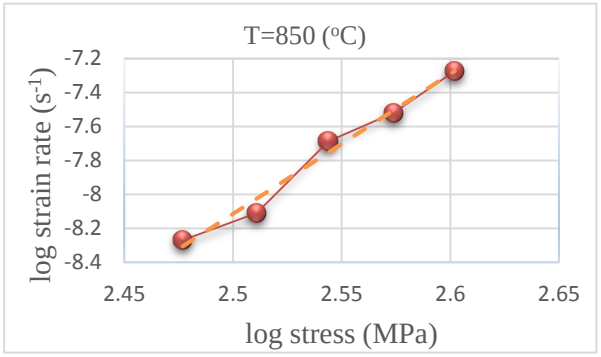

Figure 4. The linearity gradient line of the Norton equation in the spherical pressure vessel at 850 °C

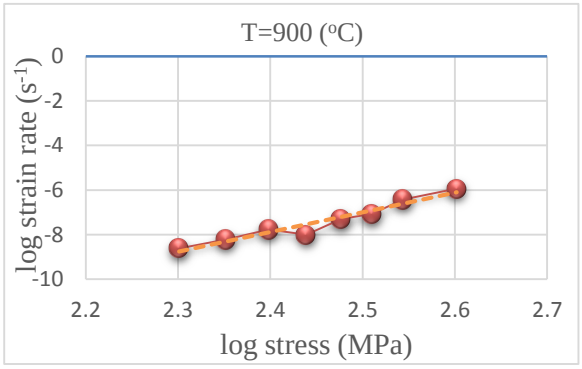

Figure 5. The linearity gradient line of the Norton equation in the spherical pressure vessel at 900 °C

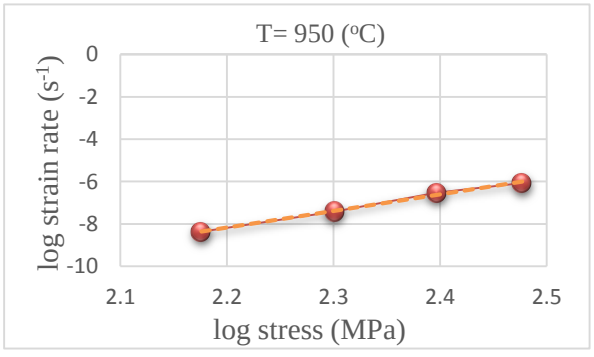

Figure 6. The linearity gradient line of the Norton equation in the spherical pressure vessel at 950 °C

From the Eq. (9) for Figures 3-6, line equation and coefficients B and *n* are shown in Table 6.

Table 6. Line equation, coefficients B and *n* for Figures 3-6

No. Figure	Line equation	Coefficient B	*n*
3	$y = 6.987x\text{-}26.676$	$10^{-26.676}$	6.9870
4	$y=8.2507x\text{-}28.742$	$10^{-28.742}$	8.2507
5	$y = 8.8107x\text{-}29.031$	$10^{-29.031}$	8.8107
6	$y = 7.8169x\text{-}25.371$	$10^{-25.371}$	7.8169

After linearization and obtaining the required constant, we can obtain radial and circumferential stresses:

$$\sigma_r = \frac{p}{a^{-3/n}-b^{-3/n}}(b^{-3/n} - r^{-3/n}) \quad (10)$$

$$\sigma_\theta = \frac{p}{a^{-3/n}-b^{-3/n}}(b^{-3/n} + \frac{3-2n}{2n}r^{-3/n}) \quad (11)$$

According to the relationships between Eqs. (10) and (11) and insert them in the Norton law or the Eq. (9), we can obtain the minimum strain rate, or the equivalent creep:

$$\dot{\varepsilon}_e = B[\frac{3p}{2n(a^{-3/n}-b^{-3/n})}]^n r^{-3} \quad (12)$$

By using the above relation, we can obtain the equivalent creep in all points of the spherical vessels radius Now, for autofrettage, the spherical vessels must be taken to plastic and the equations necessary to open up the result of the Norton equations, but which include both the elastic and the plastic, have to be developed.

Regarding the hardening process, if the tensile stress reaches σ_e during plastic deformation, the resulting tension is removed and reaches to a constant value of $2\sigma_y$ as shown in Figure 7*b*. The strain-strain relation can be obtained with thermal stress coefficient (α), strain independent of heat and strain of plastic. The radial stress σ_r and the circumferential stress σ_θ must satisfy the equation of equilibrium.

As shown in Figure 7*a*, through autofrettage, part of vessel passes from the radius of r_c into the plastic region, and from that radius to the outer radius remains in the elastic region. This creates a protective layer to withstand stress. As shown in Figure 7*b*, we can see the autofrettage that makes part of the spherical vessels radius change from the elastic region to the plastic and then we removed the applied stress to restore the amount of elastic strain and at the end of the process, we have remained stress that called residual stress. It can be seen that the yield stress in the autofrettage mode, is 2 times the amount of stress in the normal state.

$$\frac{d\sigma_r}{dr} - \frac{2}{r}(\sigma_\theta - \sigma_r) = 0 \quad (13)$$

The strains compatibility equation is:

$$\frac{d\varepsilon_\theta}{dr} - \frac{\varepsilon_\theta - \varepsilon_r}{r} = 0 \quad (14)$$

The steady state temperature is determined through the symmetry of the spherical vessels as we have [28]:

$$T = T_{r_0} + (T_{r_i} - T_{r_0})\frac{r_0/r - 1}{r_0/r_i - 1} \quad (15)$$

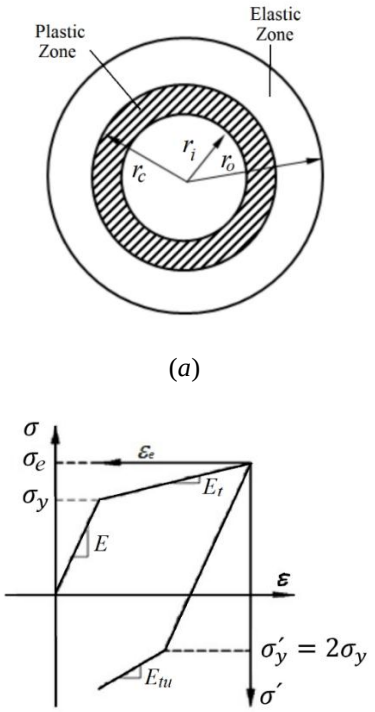

Figure 7. *a*) The Elastic and Plastic zones in the autofrettage spherical pressure vessel, *b*) The stress-strain curve considering the hardening process [28]

This research assume that the temperature inside the vessel is equal to the outside of the spherical vessel, and then the above expression (15) is equal to:

$$T = T_{r_0} = T_{r_i} \tag{16}$$

On this basis, we have to measure Von Mises yield criterion:

$$\sigma_\theta - \sigma_r = \sigma_y \tag{17}$$

For elastoplastic materials [28]:

$$\sigma_e = \sigma_y + E_p \varepsilon_e^p \tag{18}$$

Eq. (18) shows that the equivalent stress is equal to the equivalent yield stress and the term of the plastic strain is added to the equation. In the following, by pasting the plastic term in the general formula of stresses, we can satisfy the equivalent stress equation [28]:

$$E_p = \frac{E_t E}{E - E_t} \tag{19}$$

E_t is equal to the gradient of the plastic section curve in the stress-strain curve (Figure 7).

$$\varepsilon_r^p = \frac{1}{E_p}(\sigma_r - \sigma_\theta) \tag{20}$$

$$\varepsilon_\theta^p = \frac{1}{2E_p}(\sigma_\theta - \sigma_r) \tag{21}$$

Generally, for radial strain and circumferential strain with respect to plastic strains we will have:

$$\varepsilon_r = \frac{1}{E}(\sigma_r + 2v^e\sigma_\theta) + \alpha T + \varepsilon_r^p \tag{22}$$

$$\varepsilon_\theta = \frac{1}{E}((1 - v^e)\sigma_\theta + v^e\sigma_r) + \alpha T + \varepsilon_\theta^p \tag{23}$$

Clearly, v^e is equivalent Poisson ratio and α is the thermal expansion coefficient. For the elastoplastic sphere area, the general radial and circumferential strains in terms of stresses are as follows:

$$\varepsilon_{r_{aut}} = \frac{1}{E}(\sigma_r + 2v^e\sigma_\theta) + \alpha T + \frac{1}{E_p}(\sigma_r - \sigma_\theta) \tag{24}$$

$$\varepsilon_{\theta_{aut}} = \frac{1}{E}((1 - v^e)\sigma_\theta + v^e\sigma_r) + \alpha T + \frac{1}{2E_p}(\sigma_\theta - \sigma_r) \tag{25}$$

The stress-strain relations for stresses can be written in terms of α thermal expansion coefficient:

$$\sigma_{r_{aut}} = \frac{E}{(1+v^e)(1-2v^e)}\left[(1 - v^e)\left(\varepsilon_r - \alpha T - \varepsilon_r^p\right) + 2v^e\left(\varepsilon_\theta - \alpha T - \varepsilon_\theta^p\right)\right] \tag{26}$$

$$\sigma_{\theta_{aut}} = \frac{E}{(1+v^e)(1-2v^e)}\left[\left(\varepsilon_\theta - \alpha T - \varepsilon_\theta^p\right) + v^e\left(\varepsilon_r - \alpha T - \varepsilon_r^p\right)\right] \tag{27}$$

To simplify the radial and circumferential stresses, we can use the quantities σ_r^* and σ_θ^*, which are the same as non-dimensional values of radial and circumferential stresses.

$$\sigma_r^* = \frac{\sigma_{r_{nor}}}{\sigma_{r_{aut}}} \quad . \quad \sigma_\theta^* = \frac{\sigma_{\theta_{nor}}}{\sigma_{\theta_{aut}}} \tag{28}$$

3. Results and Discussion

To investigate the above-mentioned problem, at first, this spherical under pressure vessel should be checked in the normal and then in autofrettage state and the final creep with respect to stress-strain equations should be compared. Eventually obtained creep or Norton equation are compared in these two modes and the effects of autofrettage are investigated in the spherical vessel. To obtain this, we calculate the constant values of *n* and B, and then through creating relations (7) and (17) and inserting the material specification (tables. 2 and 3) in Eqs. (10), (11) and then (12) we can obtain the general creep in the non- autofrettage mode. Now, according to normal (non-autofrettage) part solution and obtaining the radial and circumferential stresses in the autofrettage mode, and also through obtaining the amount of E_P from E_t, we can calculate creep in the autofrettage mode from Norton relationship (7) and compare the results in both modes. The considerations have been in this paper. according to Table 3, the UTS amount at the maximum test temperature is 660 MPa, which is why we consider the critical pressure to be 600 MPa. Optionally we sorting pressure between 100 and 600 MPa. Due to the fact at low pressures there is no appreciable creep change, further particle splitting will be measured at close to the critical pressure. For the better comparison, the variation of σ_r^* and σ_θ^* in terms of *r* for several temperatures illustrated in Tables 7 and 8.

Table 7. The variation of σ_r^* versus radius of the vessel for several temperatures

σ_r^*	r (m)						
T (°C)	0.5	0.55	0.6	0.65	0.7	0.75	0.8
800	0.790	0.597	0.437	0.302	0.187	0.0876	0.00
850	0.807	0.606	0.442	0.305	0.188	0.0878	0.00
900	0.813	0.610	0.444	0.306	0.189	0.0878	0.00
950	0.802	0.603	0.440	0.304	0.188	0.0877	0.00

Table 8. The variation of σ_θ^* versus radius of vessel for several temperatures

σ_θ^*	r (m)						
T(°C)	0.5	0.55	0.6	0.65	0.7	0.75	0.8
800	0.470	0.629	0.702	0.744	0.772	0.791	0.806
850	0.449	0.623	0.700	0.744	0.772	0.791	0.806
900	0.441	0.621	0.700	0.744	0.772	0.791	0.806
950	0.456	0.625	0.701	0.744	0.772	0.791	0.806

These results show, that the value of σ_r^* by increasing r decrease, and at the external radius of vessel σ_r^* equal to zero. Also, increasing temperature of the vessel from 800 to 950 °C, σ_r^* slight and modest changes. And the value of σ_θ^* by increasing r increase. Also, increasing temperature of vessel from 800 to 950 °C, σ_θ^* modest changes.

To obtain creep in normal mode, according to the results, it is enough to obtain the material specification and considering Figures 3 to 6, (n; B) constant in Eq. (9). By putting these values into Eq. (12), which gives the creep equivalence with respect to the equivalent stress in the Von Mises criterion, the creep values at 100, 300, 400, 500, 525, 550, 575, and 600 at each test temperature are calculated and displayed.

To compare the present research with previous studies, the ratio of the stresses (radial, circumferential or hoop, equivalent or effective) distribution and internal pressure versus R/R_i (r/r_i) are illustrated in Figures 8 and 9.

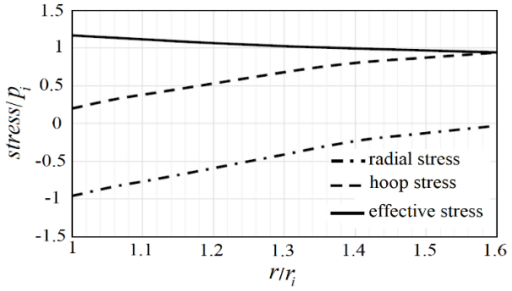

Figure 8. The ratio of the stresses distribution and internal pressure versus r/r_i

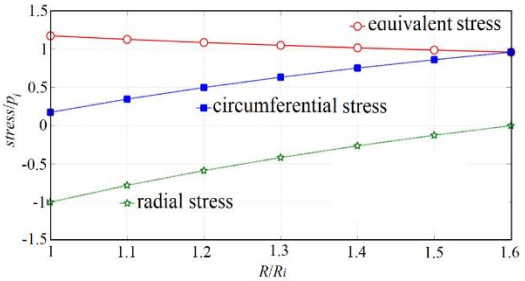

Figure 9. The ratio of the stresses distribution and internal pressure versus R/R_i

Also, the value of the stresses (Figures 8 and 9) are shown in Table 10. According to Table 9, between the results of the present research and the reference [34], which is done with the ANSYS software, there is a good compatibility between the results.

Table 9. The present work results and referenc [34], pressure equal to 70 Mpa, T=450 °C, 2.25 Cr-1 Mo Steel.

Circumferential stress/ p_i		Equivalent stress / p_i		radial stress/ p_i		R/R_i
Present work	Sorkhabi [34]	Present work	Sorkhabi [34]	Present work	Sorkhabi [34]	
0.1573	0.1746	1.1573	1.1746	-1	-1	1
0.3347	0.3469	1.1179	1.1276	-0.7832	-0.7806	1.1
0.4914	0.4983	1.0831	1.0863	-0.5917	-0.5880	1.2
0.6312	0.6326	1.0520	1.0496	-0.4208	-0.4171	1.3
0.7571	0.7529	1.0241	1.0168	-0.2670	-0.2639	1.4
0.8713	0.8615	0.9987	0.9872	-0.1274	-0.1257	1.5
0.9755	0.9603	0.9755	0.9603	0	0	1.6

In the normal mode, which there is no process except the internal stress applied, creep is shown in Figures 10 to 13, which is observed as creep start in the descending order and in a non-linear manner from the inner wall, and then in a certain amount in the outer wall will be stopped.

Figures 14 to 17 show the effect of the autofrettage process in a spherical vessel, which indicates the creep slope is more than the normal mode and from a specified radius, creep value has a sharp drop in autofrettage process.

To investigate the creep graphs in the autofrettage thick-walled spherical vessel, it is necessary to have the radial and circumferential stresses relations in the normal mode and by putting them in the autofrettage relations, we can calculate creep in the autofrettage pressure vessels.

From Eqs. (18) to (24), and embedding in Eq.(17), we can obtain both the equivalent stress in the Von Mises criterion and the creep or Norton law graphs. In order to better comparison creep due to autofrettage process, it is better to compare the stress in both the normal and the autofrettage modes at the critical pressure to observe the effect of the autofrettage process on the maximum creep at the several test temperatures. Therefore, creep rates in the thick-walled spherical vessel in critical pressure of 600 Mpa for autofrettage and normal modes (non-autofrettage) are shown in Figures 18 and 19.

Also, Maximum creep amounts in the normal and autofrettage thick-walled spherical vessels in critical pressure of 600 MPa with several temperatures illustrated in Tables 10 and 11. According to Figures 18 and 19 show that the autofrettage process makes the creep curves converge at zero at the 0.7-meter radius, while in the normal mode, this happens at lower temperatures.

Also, the creep values at several temperatures and pressures in the two modes of normal and autofrettage for thick-walled spherical vessel illustrated in Tables 12 and 13. As it was mentioned at the beginning of the article, data were obtained from experiments at the University of Swansea in England, where temperatures of 800 °C was initial and 950 °C was the final temperature for the operation.

Table 10. Maximum creep amounts in the normal thick-walled spherical Vessel in critical pressure of 600 MPa with several temperatures

T ($C°$)	800	850	900	950
$\dot{\varepsilon}_e$	$1.68*10^{-7}$	$5.05*10^{-6}$	$9.6*10^{-5}$	$7.15*10^{-4}$

Table 11. Maximum creep amounts in the autofrettage thick-walled spherical vessel in critical pressure of 600 MPa and several temperatures

T ($C°$)	800	850	900	950
$\dot{\varepsilon}_e$	$2.50*10^{-8}$	$6.0*10^{-7}$	$1.0*10^{-5}$	$9.0*10^{-5}$

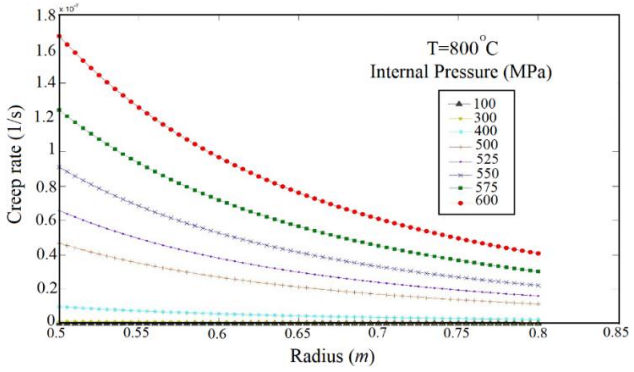

Figure 10. The creep in the normal thick-walled spherical vessel at 800°C

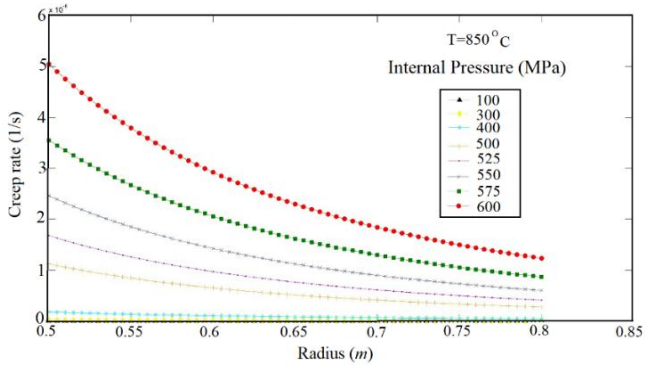

Figure 11. The creep in the normal thick-walled spherical vessel at 850°C

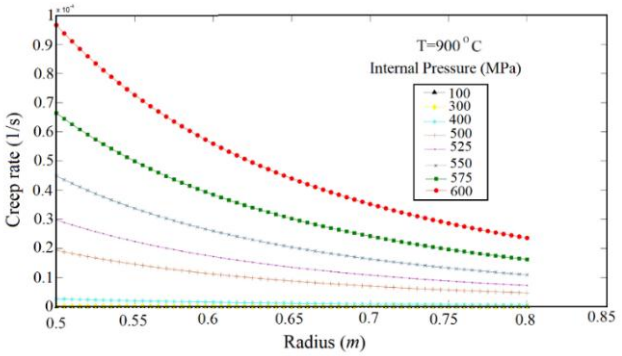

Figure 12. The creep in the normal thick-walled spherical vessel at 900°C

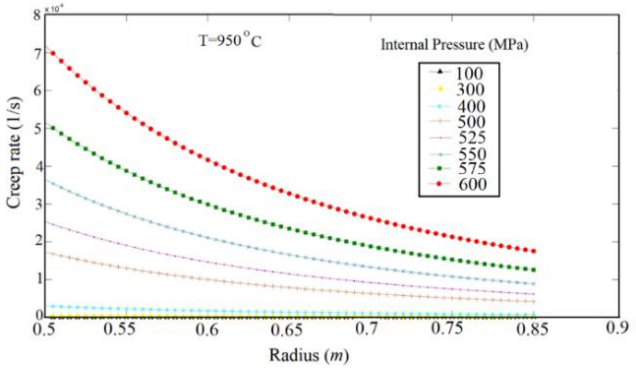

Figure 13. The creep in the normal thick-walled spherical vessel at 950°C

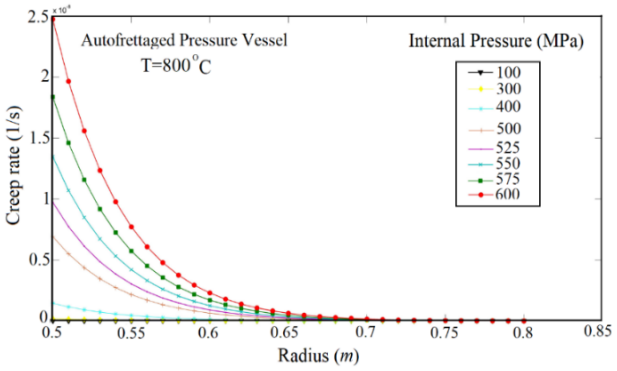

Figure 14. The creep in the autofrettage thick-walled spherical vessel at 800°C

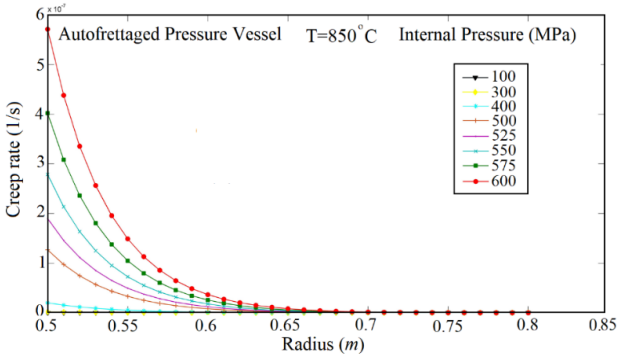

Figure 15. The creep in the autofrettage thick-walled spherical vessel at 850 °C

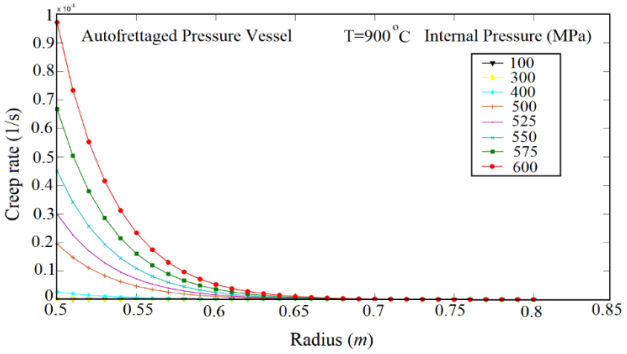

Figure 16. The creep in the autofrettage thick-walled spherical vessel at 900 °C

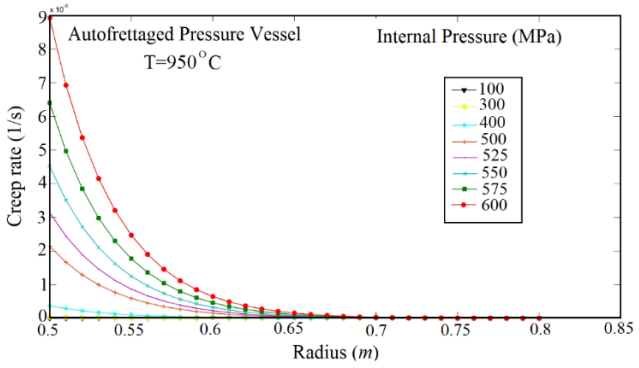

Figure 17. The creep in the autofrettage thick-walled spherical vessel at 950 °C

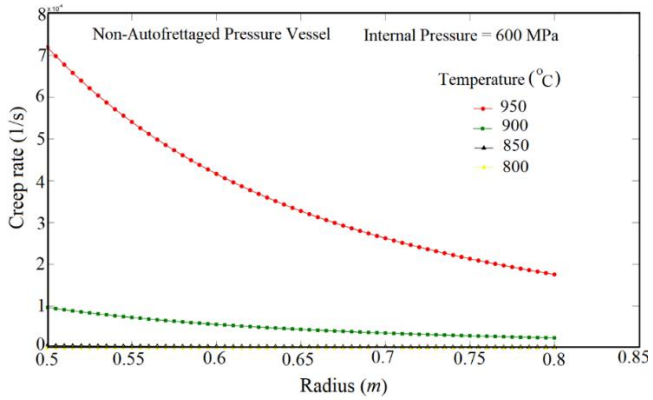

Figure 18. The creep of the normal thick-walled spherical vessel in critical pressure of 600 Mpa

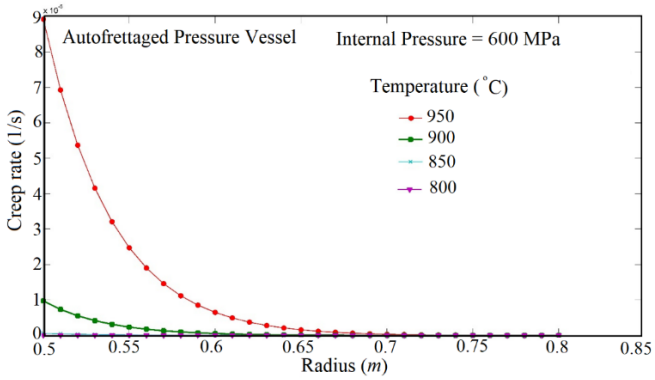

Figure 19. The creep in the autofrettage thick-walled spherical vessel in critical pressure of 600 Mpa

Table 12. The creep values at several temperatures and pressures in the normal vessel (Non-Autofrettage Vessel)

Creep (1/s)				*r*(*m*)				
T (°C)	p (MPa)	0.5	0.55	0.6	0.65	0.7	0.75	0.8
800	100	6.12E-13	4.60E-13	3.54E-13	2.79E-13	2.23E-13	1.81E-13	1.49E-13
	300	1.32E-09	9.91E-10	7.64E-10	6.01E-10	4.81E-10	3.91E-10	3.22E-10
	400	9.85E-09	7.40E-09	5.70E-09	4.48E-09	3.59E-09	2.92E-09	2.40E-09
	500	4.68E-08	3.52E-08	2.71E-08	2.13E-08	1.71E-08	1.39E-08	1.14E-08
	525	6.58E-08	4.95E-08	3.81E-08	3.00E-08	2.40E-08	1.95E-08	1.61E-08
	550	9.11E-08	6.85E-08	5.27E-08	4.15E-08	3.32E-08	2.70E-08	2.23E-08
	575	1.24E-07	9.34E-08	7.20E-08	5.66E-08	4.53E-08	3.68E-08	3.04E-08
	600	1.67E-07	1.26E-07	9.69E-08	7.62E-08	6.10E-08	4.96E-08	4.09E-08
850	100	1.92E-12	1.44E-12	1.11E-12	8.73E-13	6.99E-13	5.68E-13	4.68E-13
	300	2.66E-08	1.25E-08	9.59E-09	7.55E-09	6.04E-09	4.91E-09	4.05E-09
	400	1.78E-07	1.34E-07	1.03E-07	8.10E-08	6.49E-08	5.27E-08	4.35E-08
	500	1.12E-06	8.43E-07	6.49E-07	5.11E-07	4.09E-07	3.32E-07	2.74E-07
	525	1.68E-06	1.26E-06	9.71E-07	7.64E-07	6.11E-07	4.97E-07	4.10E-07
	550	2.46E-06	1.85E-06	1.43E-06	1.12E-06	8.98E-07	7.30E-07	6.01E-07
	575	3.55E-06	2.67E-06	2.06E-06	1.62E-06	1.30E-06	1.05E-06	8.68E-07
	600	5.05E-06	3.79E-06	2.99E-06	2.30E-06	1.84E-06	1.50E-06	1.23E-06
900	100	1.35E-11	1.01E-11	7.79E-12	6.13E-12	4.91E-12	3.99E-12	3.29E-12
	300	2.15E-07	1.62E-07	1.25E-07	9.80E-08	7.85E-08	6.38E-08	5.26E-08
	400	2.72E-06	2.04E-06	1.57E-06	1.24E-06	9.90E-07	8.05E-07	6.63E-07
	500	1.94E-05	1.46E-05	1.12E-05	8.83E-06	7.07E-06	5.75E-06	4.74E-06
	525	2.98E-05	2.24E-05	1.73E-05	1.36E-05	1.09E-05	8.83E-06	7.28E-06
	550	4.49E-05	3.37E-05	2.60E-05	2.04E-05	1.64E-05	1.33E-05	1.10E-05
	575	6.64E-05	4.99E-05	3.85E-05	3.02E-05	2.42E-05	1.97E-05	1.62E-05
	600	9.67E-05	7.26E-05	5.59E-05	4.40E-05	3.52E-05	2.86E-05	2.36E-05
950	100	5.95E-10	4.47E-10	3.44E-10	2.71E-10	2.17E-10	1.76E-10	1.45E-10
	300	3.19E-06	2.40E-06	1.85E-06	1.45E-06	1.16E-06	9.46E-07	7.79E-07
	400	3.02E-05	2.27E-05	1.75E-05	1.38E-05	1.10E-05	8.96E-06	7.38E-06
	500	1.73E-04	1.30E-04	1.00E-04	7.88E-05	6.31E-05	5.13E-05	4.23E-05
	525	2.53E-04	1.90E-04	1.47E-04	1.15E-04	9.24E-05	7.51E-04	6.19E-05
	550	3.65E-04	2.74E-04	2.11E-04	1.66E-04	1.33E-04	1.08E-04	8.90E-05
	575	5.16E-04	3.88E-04	2.99E-04	2.35E-04	1.88E-04	1.53E-04	1.26E-04
	600	7.20E-04	5.41E-04	4.17E-04	3.28E-04	2.62E-04	2.13E-04	1.76E-04

Table 13. The creep values at several temperatures and pressures in the normal vessel (Autofrettage Vessel)

Creep (1/s)					*r*(*m*)			
T (°C)	p (MPa)	0.5	0.55	0.6	0.65	0.7	0.75	0.8
800	100	9.05E-14	2.82E-14	8.40E-15	2.32E-15	5.75E-16	1.21E-16	2.01E-17
	300	1.95E-10	6.09E-11	1.81E-11	5.00E-12	1.24E-12	2.61E-13	4.34E-14
	400	1.46E-09	4.54E-10	1.35E-10	3.73E-11	9.25E-12	1.95E-12	3.24E-13
	500	6.92E-09	2.16E-09	6.42E-10	1.78E-10	4.40E-11	9.28E-12	1.54E-12
	525	9.74E-09	3.04E-09	9.03E-10	2.50E-10	6.18E-11	1.31E-11	2.17E-12
	550	1.35E-08	4.20E-09	1.25E-09	3.45E-10	8.56E-11	1.81E-11	3.00E-12
	575	1.84E-08	5.73E-09	1.71E-09	4.71E-10	1.17E-10	2.46E-11	4.09E-12
	600	2.48E-08	7.72E-09	2.30E-09	6.34E-10	1.57E-10	3.32E-11	5.50E-12
850	100	2.17E-13	5.66E-14	1.39E-14	3.14E-15	6.20E-16	1.02E-16	1.26E-17
	300	1.88E-09	4.89E-10	1.20E-10	2.71E-11	5.36E-12	8.79E-13	1.09E-13
	400	2.01E-08	5.25E-09	1.30E-09	2.91E-10	5.75E-11	9.43E-12	1.17E-12
	500	1.27E-07	3.31E-08	8.14E-09	1.83E-09	3.63E-10	5.95E-11	7.36E-12
	525	1.90E-07	4.95E-08	1.22E-08	2.74E-09	5.43E-10	8.89E-11	1.10E-11
	550	2.79E-07	7.27E-08	1.79E-08	4.03E-09	7.96E-10	1.31E-10	1.62E-11
	575	4.02E-07	1.05E-07	2.58E-08	5.81E-09	1.15E-09	1.88E-10	2.33E-11
	600	5.71E-07	1.49E-07	3.67E-08	8.25E-09	1.63E-09	3.68E-10	3.31E-11
900	100	1.35E-12	3.26E-13	7.37E-14	1.52E-14	2.72E-15	3.98E-16	4.32E-17
	300	2.17E-08	5.21E-09	1.18E-09	2.42E-10	4.34E-11	6.36E-12	6.91E-13
	400	2.73E-07	6.57E-08	1.49E-08	3.06E-09	5.48E-10	8.02E-11	8.72E-12
	500	1.96E-06	4.69E-07	1.06E-07	2.18E-08	3.91E-09	5.73E-10	6.23E-11
	525	3.00E-06	7.22E-07	1.63E-07	3.36E-08	6.01E-09	8.81E-10	9.57E-11
	550	4.42E-06	1.09E-06	2.46E-07	5.60E-08	9.05E-09	1.33E-09	1.44E-10
	575	6.70E-06	1.61E-06	3.64E-07	7.48E-08	1.34E-08	1.96E-09	2.13E-10
	600	9.72E-06	2.34E-06	5.30E-07	1.09E-07	1.95E-08	2.86E-09	3.10E-10
950	100	7.38E-11	2.05E-11	5.37E-12	1.30E-12	2.77E-13	4.96E-14	6.78E-15
	300	3.95E-07	1.09E-07	2.88E-08	6.96E-09	1.49E-09	2.67E-10	3.64E-11
	400	3.75E-06	1.04E-06	2.73E-07	6.60E-08	1.41E-08	2.52E-09	3.45E-10
	500	2.15E-05	5.95E-06	1.56E-06	3.78E-07	8.07E-08	1.44E-08	1.98E-09
	525	3.14E-05	8.71E-06	2.29E-06	5.53E-07	1.18E-07	2.11E-08	2.90E-09
	550	4.52E-05	1.25E-05	3.29E-06	7.95E-07	1.70E-07	3.04E-08	4.16E-09
	575	6.40E-05	1.77E-05	4.66E-06	1.13E-06	2.41E-07	4.30E-08	5.89E-09
	600	8.93E-05	2.48E-05	6.50E-06	1.57E-06	3.36E-07	6.00E-08	8.21E-09

4. Conclusions

Due to the nature of the creep, which is affected by the material, environmental and mechanical conditions, it can be concluded that by changing the type of processes, different results of the creep can be obtained.

In the normal mode, which there is no process except the internal stress applied, creep is shown in Figures 10 to 13, which is observed as creep start in the descending order and in a non-linear manner from the inner wall, and then in a certain amount in the outer wall will be stopped. The spherical vessel elasticity makes the creep slope in the diagram seems less in the far lower pressure. Now, through considering the autofrettage process applied, as well as maintaining the environmental and mechanical conditions like normal mode, we can examine the creep completely.

According to the process of autofrettage, which causes a part of the elastic region to turn into the plastic one in spherical vessels, naturally, the amount of creep at any temperature and pressure should be less than the corresponding one in the non-autofrettage case. Because of entering the plastic zone and then removing the applied force, some amount of strain in the spherical vessels will remain, so the external force which is supplied by both internal pressure and temperature and by maintaining mechanical and thermal conditions like non-autofrettage state will not be able to produce a creep in accordance with non-autofrettage creep.

Figures 14 to 17 show the effect of the autofrettage process in a spherical vessel, which indicates the creep slope is more than the normal mode and from a specified radius, creep value has a sharp drop in autofrettage process. According to the pressure 600 MPa, which is a critical pressure at 950 °C, and it applied at various temperatures and comparison normal and autofrettage modes with each other, it is shown in Figures 18 and 19, the equivalent creep in the entire pressure vessel which depends on the test temperatures decreases by at least 10 times.

It can be concluded the temperature plays an important role in increasing the creep in the thick-walled spherical pressure vessel, in which with increasing temperature the curve slope will increase. According to Tables 12 and 13, it can be noticed at low pressures (such as 100 MPa), the creep amount is very low and whenever autofrettage mode applies, this amount will be even lower. Generally,

Tables 12 and 13 show (in the same radius in both modes), the creep amount in the autofrettage mode is less 10 times at an internal radius and less 10^5 times in the external radius than normal mode. It is also possible to examine the effect of temperature on the creep in the respective radius .it can be observed in the Tables 12 and 13 the creep exact amount according to the temperature factors and pressure in two cases of autofrettage and normal modes.

Finally, it can be concluded applying the autofrettage process in nickel super-alloyed thick-walled spherical pressure vessel, not only it reduces the creep amount by at

least 10 times the internal radius, but we can fix this amount at a certain radius and even it can be much less than normal mode at the same radius. By comparing creep values in the normal mode with the creep value after applying autofrettage, we can observe that the autofrettage of spherical vessels is a very practical process in the prevention and immunization of thick-walled spherical vessels, so that it can control or eliminate destructive actions such as creep.

According to Table 9, between the results of the present research and the reference [34], which is done with the ANSYS software, there is a good compatibility between the results.

References

[1] K. Zaba, S. Puchlerska, M. Kwiatkowski, M. Nowosielski, M. Glodzik, T. Tokarski, P. Seibt, Comparative analysis of microstructure of the plastically deformed alloy Inconel®718, manufactured by plastic working and Direct Metal Laser Sintering., Arch. Metall. Mater 61(2016)143–148.

[2] N.S. Bhatnagar, P. Kularni, V.K. Arya, Primary creep analysis of an anisotropic thick-walled spherical shell. ASME J. Pressure Vessel Technol 109 (1987) 347–351.

[3] G.K. Miller, Stresses in a spherical pressure vessel undergoing creep and dimensional changes. Int. J. Solids Struct 32 (1995) 2077–2093.

[4] A. Nayebi, R. El Abdi, Cyclic plastic and creep behavior of pressure vessels under thermomechanical loading. Compute. Mater. Sci 25 (2002) 285–296.

[5] V. Gray, Z. Abdallah, M.T. Whittaker, Creep models: determining the parameters and constants of failure. Swansea University (2015) 1–29.

[6] L.H. You, H. Ou, Steady-state creep analysis of thick-walled spherical pressure vessels. ASME J. Pressure Vessel Technol 128 (2008) 1–5.

[7] A.P. Parker, Autofrettage of open end tubes-pressures, stresses, strains and code comparisons. ASME J. Pressure Vessel Technol 123 (2001) 271–281.

[8] P. Livieri, P. Lazzarin, Autofrettage cylindrical vessels and bauschinger effect: an analytical frame for evaluating residual stress distributions. ASME J. Pressure Vessel Technol 124 (2002) 38–46.

[9] R. Thumser, J.W. Bergmann, M.Vormwald, Residual stress fields and fatigue analysis of autofrettage parts. International Journal of Pressure Vessel and piping 79 (2002) 113–117.

[10] A.P. Parker, A re-autofrettage procedure for mitigation of bauschinger effect in thick cylinders. ASME J. Pressure Vessel Technol 126 (2004) 451–454.

[11] X.P. Huang, W.C. Cui, Effect of bauschinger effect and yield criterion on residual stress distribution of autofrettage tube. ASME J. Pressure Vessel Technol 128 (2006) 212–216.

[12] A.P. Parker, X. Huang, Autofrettage and re-autofrettage of a spherical pressure vessel. Journal of Pressure Vessel Technology 129 (2007) 83–88.

[13] B.A. Boley, J.H. Weiner, Theory of thermal stresses. New York: John Wiley, 1960.

[14] W. Nowaki, Thermo-elasticity. Oxford, Pergamon Press, 1965.

[15] S. Timoshenko, J.N. Goodier, Theory of elasticity. New York, McGraw-Hill, 1951.

[16] W. Johnson, P.B. Mellor, Engineering plasticity. London, Ellis Horwood, 1983.

[17] E. Whalley, The design of pressure vessels subjected to thermal Stress-I, general theory for monoblock vessels. Can J Technol 34 (1956) 268–75.

[18] J.R. Cowper, The elastoplastic thick-walled sphere subjected to a radial temperature gradient. Trans ASME 27 (1960) 496–500.

[19] M.G. Derrington, W. B. Johnson, The onset of yield in a thick spherical shell subject to internal pressure and a uniform heat flow. Appl Sci Res Ser A7 (1958) 408–414.

[20] W. Johnson, P.B. Mellor, Elastic-plastic behavior of thick-walled spheres of non-work-hardening material subject to a steady state radial temperature gradient. Int J Mech Sci 4 (1961) 147–54.

[21] M.H. Kargarnovin, A.R. Zarei, H. Darijani, Wall thickness optimization of thick-walled spherical vessel using thermo-elastoplastic concept. International Journal of Pressure Vessels and Piping 82 (2005) 379–385.

[22] M. Davoudi Kashkoli, M. Zamani Nejad, Time- dependent Thermo-elastic creep analysis of thick-walled spherical pressure vessels made of Functionally Graded Materials, Journal of Theoretical and applied Mechanics 53 (4) (2015) 1053–1065.

[23] A. Gharechaei, A. Loghman, Analysis of creep stress and strain histories in an autofrettage thick-walled sphere,Thesis for Degree of Master of Science (M.SC) in Mechanical Engineering. The Mechanical Engineering Department of Solid Mechanics, University of Kashan, 2014.

[24] A. Loghman1, H. Tourang, Non-stationary electro- thermo-mechanical creep response and smart deformation control of thick-walled sphere made of polyvinylidene fluoride, J Braz. Soc. Mech. Sci. Eng 38 (2016) 2547–2561.

[25] A. Loghman, A. Ghorbanpour Arani S. M. A. Aleayoub, Time-dependent creep stress redistribution analysis of thick-walled functionally graded spheres, Mechanics of Time-Dependent Materials 15 (2011) 353–365.

[26] Y. Liu, N.J. Shen, The residual stress and strain solutions of autofrettaged pressure vessels with a cone and cylinder connection, Journal of Stress Analysis 27 (1992) 7–14.

[27] Atlas of stress-strain curves. ASM international, the materials information society, second edition, 2002.

[28] S.C.M. Rupali, S. Susenjit, Finite Element Analysis of Thermally Autofrettage Strain-Hardening Spherical Vessels. Internal Journal of Research in Economics and Social Sciences (IJRESS) 7 (2017) 272–280.

[29] G.E. Wasielewski, Nickel-Base Super Alloy Oxidation, Interim Progress Report #2, Air Force. Contract No. AF33 (615)-2861 for Research and Technology Division, Air Force Systems Command USAF by MDL-FPD General Electric, Cincinnati, Ohio, 1967.

[30] M.J. Fleetwood, P.J. Penrice, J.E. Whittle, Thermal- Fatigue Resistance of Cast Nickel-Base High Temperature Alloys, Foundry Trade Journal (2001) 657–667.

[31] M.J. Donachie, S.J. Donachie, Super alloys: A Technical Guide, ASM International, Second Edition, 2002.

[32] L. N. Moskowitz, Regis Pelloix, N. J. Grant, Properties of IN-100 Processed by Powder Metallurgy, 1972, DOI: 10.7449/1972/Superalloys_1972_Z-1_Z-25.

[33] W. B. Jensen, The Universal Gas Constant R, J. Chem Educ 80 (2003) 731–732.

[34] A.M. Sorkhabi, R. Fard-Moradinia, Numerical study of stress redistribution in thick-walled spherical vessel under pressure and high temperature, 2nd International Conference on Mechanical and Aerospace Engineering, May 11, Tehran, Iran, (2017). (In Persian).